Acta Neuropathol (2005) 109: 457–466
DOI 10.1007/s00401-004-0971-7

REGULAR PAPER

**Yorito Anamizu · Hiroshi Kawaguchi · Atsushi Seichi
Shinji Yamaguchi · Emiko Kawakami · Naotoshi Kanda
Shiro Matsubara · Makoto Kuro-o · Yoichi Nabeshima
Kozo Nakamura · Kiyomitsu Oyanagi**

Klotho insufficiency causes decrease of ribosomal RNA gene transcription activity, cytoplasmic RNA and rough ER in the spinal anterior horn cells

Received: 8 September 2004 / Revised: 29 November 2004 / Accepted: 29 November 2004 / Published online: 16 April 2005

Abstract The *klotho* gene was identified in 1997 as the gene whose severe insufficiency (*kl*/*kl*) causes a syndrome resembling human aging, such as osteoporosis, arteriosclerosis, gonadal atrophy, emphysema, and short life span in a mouse strain. Regarding the gait disturbance reported in *kl*/*kl* mice, the present study examined the spinal cord of *kl*/*kl* mice, and revealed decreases in the number of large anterior horn cells (AHCs), the amount of cytoplasmic RNA, the number of ribosomes and rough endoplasmic reticulum (rER), and the activity of ribosomal (r) RNA gene transcription without significant loss of the total number of neurons in the ventral gray matter. Increased immunostaining of phosphorylated neurofilament in the AHCs and of glial fibrillary acidic protein in reactive astrocytes in the anterior horn of *kl*/*kl* mice were also observed. On the other hand, the posterior horn was quite well preserved. The results suggest that the *kl*/*kl* insufficiency causes atrophy and dysfunction of the spinal AHCs through decreased activity of rRNA gene transcription, which may reduce the amount of cytoplasmic RNA and the number of ribosomes and rER. These findings resemble those found in the spinal cord of patients with classic amyotrophic lateral sclerosis (ALS). The results show that *klotho* gene insufficiency causes dysfunction of the protein synthesizing system in the AHCs, and might indicate the *klotho* gene is involved in the pathological mechanism of classic ALS. The *kl*/*kl* is a new animal model of AHC degeneration, and may provide clues to understanding the etiology of classic ALS.

Keywords Anterior horn cell · Cytoplasmic RNA · Klotho · Ribosomal RNA gene · Transcription activity

Y. Anamizu · E. Kawakami · K. Oyanagi (✉)
Department of Neuropathology,
Tokyo Metropolitan Institute for Neuroscience,
2-6 Musashidai, Fuchu, 183-8526 Tokyo, Japan
E-mail: k123ysm@tmin.ac.jp
Tel.: +81-42-3253881 ext 4711
Fax: +81-42-3218678

Y. Anamizu · H. Kawaguchi · A. Seichi · K. Nakamura
Department of Orthopedic Surgery,
Graduate School of Medicine,
University of Tokyo, Tokyo, Japan

S. Yamaguchi
Department of Biochemistry,
Molecular Biology and Cell Biology, Northwestern University,
Evanston, Illinois, USA

N. Kanda
Department of Anatomy,
Graduate School of Veterinary Medicine,
Tokyo University of Agriculture and Technology,
Tokyo, Japan

S. Matsubara
Department of Neurology,
Tokyo Metropolitan Neurological Hospital,
Fuchu, Tokyo, Japan

M. Kuro-o
Department of Pathology,
University of Texas Southwestern Medical Center,
Dallas, Texas, USA

Y. Nabeshima
Department of Tumor Biology,
Graduate School of Medicine, Kyoto University,
Kyoto, Japan

Introduction

Mouse lines exhibiting symptoms of early-onset senescence have been established using insertion mutations; it has been shown that the absence of a single gene produces a variety of aging symptoms. The *klotho* gene has been identified as the causal gene at 5G3 in mice and 13q12 in humans [27]. Homozygotes with the *klotho* gene mutation (*kl*/*kl*) are reported to demonstrate phenotypes highly similar to human aging, including osteoporosis, calcification of articular cartilage and soft tissue, arteriosclerosis, decreased activity, emphysema,

and gonadal, thymic, and dermal atrophy. The life span is reported to be 8–9 weeks on average. The *kl*/*kl* mice are senescence-accelerated mice satisfying 7 among 21 of the pathophysiological and cellular criteria of aging [27]. An association between the allele of the functional variant of the *klotho* gene and occult coronary artery disease has been reported [3].

In addition to the above-mentioned symptoms, *kl*/*kl* mice exhibit an abnormal gait. Reduction in the number of cerebellar Purkinje cells [27] may be a factor relating to the gait disturbance, but the spinal cord has not been examined genetically or histologically. To date, there have been no reports on the expression of the *klotho* gene in the spinal cord. An age-related reduction of the number of small neurons in the anterior horn has been reported in humans [25, 26, 40], and it was thus important to examine whether or not similar changes occur in *kl*/*kl* mice. The purpose of the present study was to clarify the genetic, histological, quantitative and ultrastructural peculiarities in the spinal cord in *kl*/*kl* mice, and compare those with the findings in the human spinal cord in aging. We have found some degenerative changes, similar to those reported in the human anterior horn cells (AHCs) with neurodegenerative diseases including classic amyotrophic lateral sclerosis (ALS), in this senescence model mouse.

Materials and methods

Animals

All animals were bred and kept in a breeder (Clea-Japan Corp., Tokyo, Japan) until just before the sacrifice. At sacrifice, adequate measures were taken to minimize pain and discomfort to the animals, according to the ''Guidelines for Experiments of the Tokyo Metropolitan Institute for Neuroscience''. All animal experiments conformed to the United States Public Health Service's Policy on Human Care and Use of Laboratory Animals.

The genetic background of the original *klotho* mice was a mixture of C57BL/6J and C3H/J species. We used 21 male *kl*/*kl* mice and 19 male wild-type (WT) mice at the age of 7 weeks, the period assumed to be that just before death. Genotypes of the sacrificed mice were determined by Southern blot analyses using their tails and probes to detect the inserted plasmid located adjacent to the *klotho* gene locus. The body and brain weights were measured at the time of sacrifice (Table 1).

Table 1 The body and brain weight of *kl*/*kl* and WT mice at the age of 7 weeks. Values represent mean ± SD (*kl*/*kl* homozygotes with the *klotho* mutation, *WT* wild-type)

	Body weight (g)	Brain weight (g)
kl/*kl* (male,$n=17$)	7.6 ± 1.1*	0.37 ± 0.02*
WT (male,$n=17$)	24.4 ± 1.58	0.47 ± 0.03

*$P < 0.0001$

Animals were deeply anesthetized with ether before the processing. For reverse transcription (RT)-PCR, the cervical spinal cords from *kl*/*kl* and WT mice ($n=2$, respectively) were taken up in lysis buffer for the isolation of total RNA (RNeasy kit; Qiagen, Chatsworth, CA). Fifteen *kl*/*kl* and 13 WT male mice were transcardially perfused with 4% paraformaldehyde (PFA) in 0.1 M phosphate buffer (PB) (pH 7.3) for paraffin embedding. Four *kl*/*kl* and 4 WT mice were transcardially perfused with 2.5% glutaraldehyde (GA) and 1% PFA in 0.1 M cacodylate buffer (CB) (pH 7.3) for Epon embedding.

RT-PCR procedure of the spinal cord

RNA (0.3–1 μg) was dissolved in 30 μl H_2O, and the following was added: 2.5 μl 1 M TRIS (pH 7.4), 20 μl 25 mM $MgCl_2$, 2 μl RNase-free DNase (10 U/μl; Roche Molecular Biochemicals, Mannheim, Germany), and 0.5 μl RNasin (40 U/μl; Promega, Madison, WI). The mixture was incubated for 20 min at 37°C and subsequently divided into two parts. In one part, RNA was reverse-transcribed using oligo(dT) primers (Life Technologies, Rockville, MD) and Moloney murine leukemia virus reverse transcriptase (Superscript II; Life Technologies) at 45°C for 1 h. The other part was incubated in the same mixture without the enzyme and was later used as a control for DNA contamination in the PCR. The cDNA was purified (PCR purification kit; Qiagen) and used as a template for PCR in a 60-μl reaction volume containing 1× PCR buffer containing 1.5 mM $MgCl_2$ (Perkin-Elmer, Foster City, CA), 0.2 mM dNTPs, and 0.1 μM of each primer. Specific oligonucleotide primers (Life Technologies) for PCR were designed to amplify rat (GenBank accession no. AB005141) *klotho* mRNA (forward 5'-AGATGTGGCCAGCGATAGTTA-3'; reverse 5'-ACTTGACCTGACCACCGAAGT-3') [29]. A ''hot start'' was performed manually by adding 1.5 U AmpliTaq (Perkin-Elmer) after an initial incubation of 5 min at 95°C in a thermocycler (Perkin-Elmer, 9700). For each experiment the housekeeping gene glyceraldehyde-3-phosphate dehydrogenase (GAPDH) was amplified with 20 and 22 cycles to normalize the cDNA content of the samples. Equal cDNA amounts were subsequently used for the amplification of *klotho* gene. Amplification was performed for 20–40 cycles (94°C for 30 s, 50°C for 10 s, and 72°C for 90 s). The linear range of amplification was determined for each primer set. The amplicons were analyzed on a 1.5% agarose gel stained with ethidium bromide.

Histological and immunohistochemical examination

The 5th cervical and 4th lumbar segments were removed from the 4% PFA-fixed spinal cords under a dissecting microscope. Tissue blocks were dehydrated in ethanol

series, and embedded in paraffin. Serial transverse sections (6 μm thick) were made, and were subjected to hematoxylin-eosin, Klüver-Barrera (K-B) and pyronin Y preparation.

Sections, 6 μm thick, were also subjected to immunohistochemical staining using the avidin-biotin-peroxidase complex (ABC) method with a Vectastain ABC kit (Vector, Burlingame, CA). The primary antibodies used were rabbit anti-cow ubiquitin polyclonal antibody (dilution 1:150; Dakopatts, Glostrup, Denmark), SMI-31 monoclonal antibody (dilution 1:1,000; Sternberger Monoclonals, Baltimore, MD), and rabbit anti-glial fibrillary acidic protein (GFAP) polyclonal antibody (dilution 1:1,000; Dakopatts). Lectin histochemistry for microglia was performed using IB4 coupled to horseradish peroxidase (HRP) (dilution 1:100, Sigma, St. Louis, MO). Antigenicity was increased for ubiquitin immunostaining by pretreating the sections with 0.025% trypsin for 15 min at room temperature. Endogenous peroxidase activity was quenched by incubating the sections in 3% hydrogen peroxide in methanol and then blocked by incubating for 1 h with 3% normal goat or mouse serum in phosphate-buffered saline (PBS). The sections were incubated with the required primary antibody overnight at 4°C, then incubated with the secondary reagent containing biotinylated anti-rabbit or anti-mouse IgG (diluted 1:200) for 2 h, and finally with the ABC solution for 1 h. The sections were subjected to the peroxidase reaction using freshly prepared 0.02% 3,3'-diaminobenzidine-tetrahydrochloride and 0.005% hydrogen peroxide in 0.05 M TRIS-HCl buffer pH 7.6 for 10 min at room temperature. As antibody controls, the primary antisera were either omitted or replaced with normal rabbit or mouse serum. Several specimens of neural and non-neural tissue from the patients served as positive or negative tissue controls.

Quantitative examination of the neurons in the ventral spinal gray matter

The number and sectional area of the neurons with nucleus in the ventral part (ventral side of the central canal level; which includes roughly laminae VII, VIII and IX of Rexed's [33] of the 5th cervical gray matter) were examined in three K-B-stained 6-μm-thick sections (12-μm apart to avoid double counting of the neurons) on both sides in 11 *kl*/*kl* and 10 WT mice. Neurons were identified by the presence of Nissl substance and prominent nucleoli. Sectional neuronal area including cytoplasm and nucleus was measured by a digitizer (Measure 5; System Supply, Nagano, Japan). The number of neurons examined was 2,354 in *kl*/*kl* and 2,110 in WT mice. The frequency distribution of the cell areas by 40-μm^2 increments was obtained. Abercrombie's correction factor [1] was applied for split cell error counting. We defined AHCs here as large neurons with a cell area greater than 400 μm^2, on the basis of their neuronal features and prominent nucleolus in the ventral part of the gray matter.

Measurement of diameter of nucleoli of neurons in the ventral spinal gray matter

Light microscopic black and white pictures of neurons in the ventral spinal gray matter were taken at 200-fold magnification using K-B-stained 5th cervical segments. The film negatives were magnified 19-fold with a microscopy reader RF-3A (Fuji Film corp. Tokyo, Japan) and diameters of the nucleoli on the screen were measured with the ruler of the microscopy reader. In total, 94 neurons in three *kl*/*kl* and 87 neurons in three WT mice were examined. The frequency distribution by 0.3-μm increments was obtained.

Amount of cytoplasmic RNA in the AHCs

The cytoplasmic RNA content was measured in AHCs with nucleolus by the integrated OD of pyronin Y-stained 6-μm-thick sections. The measurement of the pyronin Y-stained area with an image analyzer has been reported as a reliable method for quantitative assessment of RNA [36]. Integrated OD was measured in the cytoplasm in a routine bright field of Zeiss Axiovert 135 with 12 bits camera (Carl Zeiss, Oberkochen, Germany) using the MetaMorph (Universal Imaging. Co., West Chester, PA, USA) software. Measurement was performed in 100 randomly distributed AHCs with nucleolus in *klotho* and WT mice each (10 AHCs/mouse,10 mice each).

Ultrastructural investigation of the AHCs

Tissue blocks of the 5th cervical cords, fixed with 3% GA-1% PFA in 0.1 M PB, were postfixed with 1% osmium tetroxide, then dehydrated through a graded ethanol series, and embedded in Epon 812. Toluidine blue-stained 1-μm-thick sections were examined using a light microscope, and ultrathin sections of the ventral part of the spinal cords were stained with lead citrate and uranyl acetate and examined using an electron microscope (H9000; Hitachi, Tokyo, Japan) at 100 kV.

Measurement of transcription activity of rRNA gene in neurons in the ventral spinal gray matter

Silver staining of nucleolar organizer region-associated proteins (AgNORs) [4, 6, 14, 18, 19, 21, 30] was used to evaluate the rRNA gene transcription activity in the neurons in the ventral gray matter in *kl*/*kl* and WT mice. PFA-fixed paraffin-embedded 6-μm-thick sections of the 5th cervical segment 12 μm apart were used for the staining.

Microscopic slides were deparaffinized with xylene, dehydrated in an alcohol series, rinsed with tap water, then stained with a 1:2 blended solution of freshly prepared: (i) 2% gelatin in 1% aqueous formic acid and (ii) 50% silver nitrate solution in deionized and distilled water (DDW). The slides were incubated at 37°C in darkness for 20 min, rinsed in DDW, dehydrated with an alcohol series and xylene, and covered with DPX. Areas of AgNOR-positive regions and the nucleus were examined by a digitizer (System Supply, Nagano, Japan), and the ratio was evaluated. Two hundred thirties neurons from four *kl*/*kl* and 156 neurons from five WT mice were examined.

Statistical evaluation

Statistical evaluation was performed using the Mann-Whitney U-test to compare the ratio between *kl*/*kl* and WT mice.

Results

Body and brain weights

The body weight of *kl*/*kl* mice aged 7 weeks was about one-third that of the WT mice, and the brain weight was about four-fifths of the WT mice (Table 1).

RT-PCR for *klotho* gene expression in the spinal cords

After 40 cycles of RT-PCR, *klotho* gene expression was seen both in WT and in *kl*/*kl* mice. The expression in *kl*/*kl* mice was quite weak but significantly positive (Fig. 1). G3PDH was used as control, and the intensities did not differ between *kl*/*kl* and WT mice. The possibility of DNA contamination as a source of amplified products was believed to be excluded, since the *klotho* gene expression was not seen in the negative control (data not shown).

Light microscopic findings of the central nervous system

The neuronal population and size of neurons in the brains of *kl*/*kl* mice did not show any apparent differences from those of the controls. The cross-sectional area of the gray and white matter of the cervical and lumbar segments of the spinal cord of *klkl* mice was smaller than that in WT mice, in spite of good preservation of the cross-sectional area (Fig. 2A, B) and the neurons of the posterior horn (Fig. 2C, D) of *kl*/*kl* mice. Large AHCs were seen more frequently in WT than in the *kl*/*kl* mice, and small neurons were seen more often in the ventral gray matter in *kl*/*kl* mice (Fig. 2E, F). In the AHCs of *kl*/*kl* mice, the amount of Nissl substance,

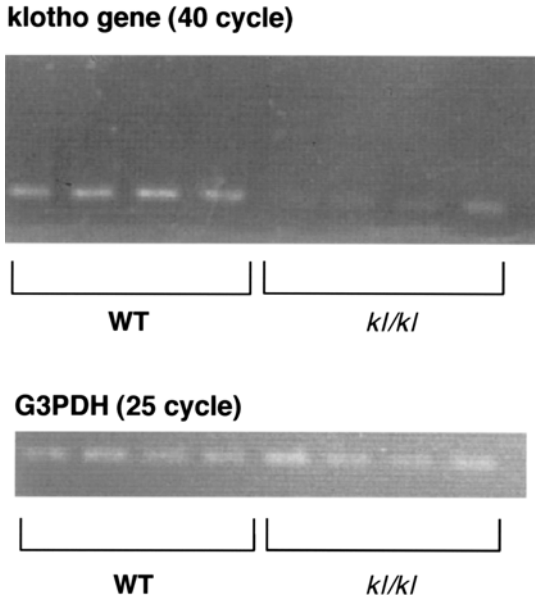

Fig. 1 *Klotho* gene expression by RT-PCR in the spinal cord. After 40 cycles of RT-PCR, *klotho* gene expression was seen in both WT and in *kl*/*kl* mice. *klotho* gene expression in *kl*/*kl* mice is quite weak but significant. G3PDH was used as control, and the intensities were not different between the two genotypes (*RT* reverse transcription, *WT* wild-type, *kl*/*kl* homozygotes with the *klotho* gene mutation)

i.e., rough endoplasmic reticulum (rER), was smaller (chromatolysis) than that in WT mice (Fig. 2G), and slight but evident accumulation of phosphorylated neurofilaments was observed (Fig. 2I, J). GFAP-immunopositive reactive gliosis was seen in the ventral horn of *kl*/*kl* mice (Fig. 2K, L), and a moderate increase of number of the IB4-positive cells was seen in the anterior horn in *kl*/*kl* mice; no significant ubiquitin-immunopositive accumulation, Bunina bodies, or spheroids were observed.

Quantitative examination of neurons in the ventral gray matter

There was no significant difference in the number of the neurons in the ventral part of the spinal gray matter between *kl*/*kl* and WT mice (Fig. 2H). However, the frequency distribution of the sectional area of the neurons in the ventral gray matter of the 5th cervical cord in the 40-μm^2 increments showed one peak at 120 μm^2 in *kl*/*kl* mice but 160 μm^2 in WT mice, indicating that the neurons in *kl*/*kl* mice were smaller (Fig. 3A). The number of large neurons with a cross-sectional area over 400 μm^2 was significantly lower in *kl*/*kl* mice than in WT ($P < 0.0001$) (Fig. 3B). The highest peaks of distribution frequency by 0.3-μm increments of the diameter of nucleoli of neurons in the ventral spinal gray matter were at 2.1–2.4 μm in *kl*/*kl* mice, but at 2.7–3.0 μm in

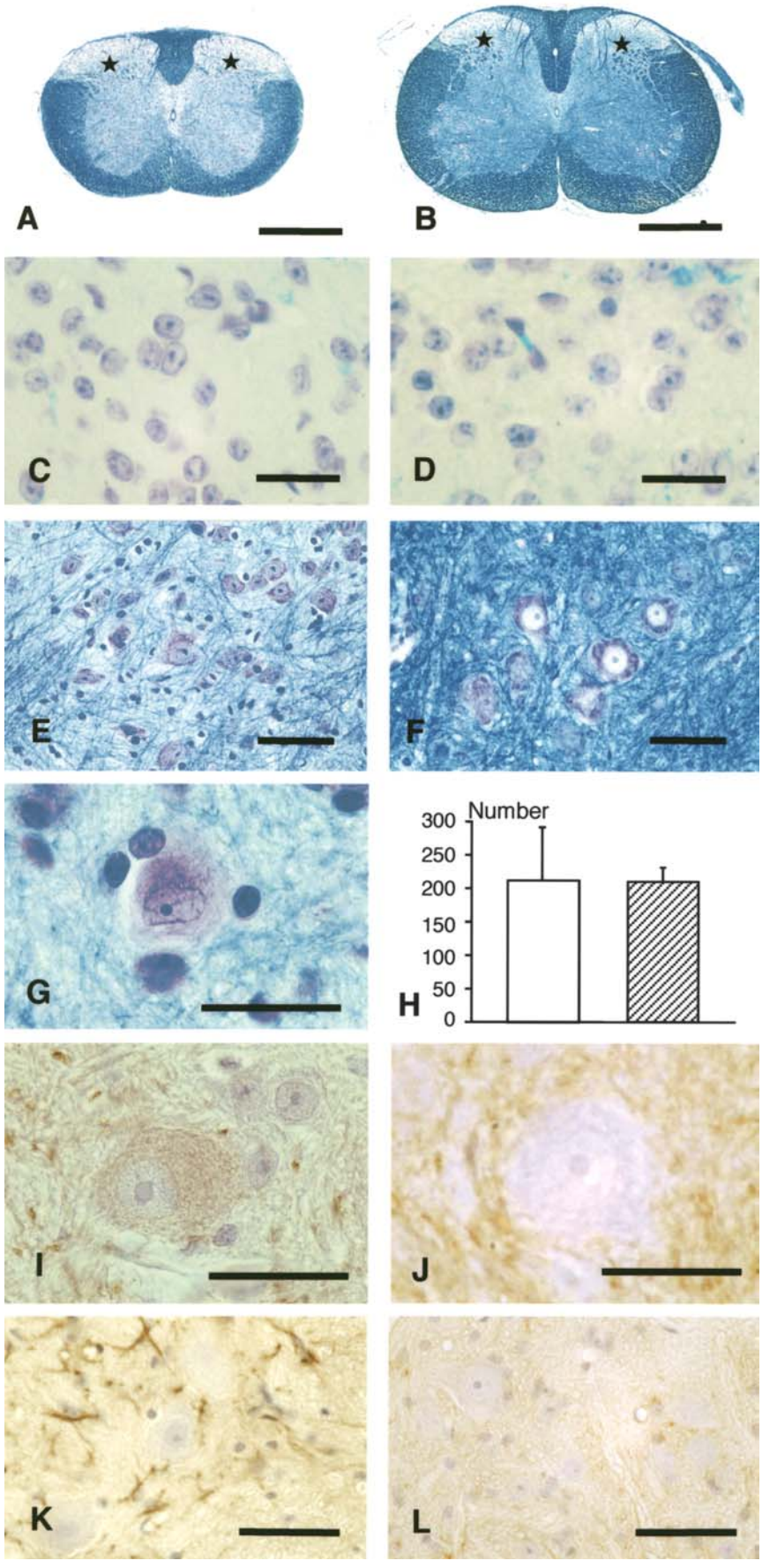

Fig. 2 Light microscopic findings of the 5th cervical spinal cord. Cross-sectional area of the gray and white matter is smaller in *kl*/*kl* mice (**A**) than in WT mice (**B**), whereas the posterior horn (*asterisk*) is well preserved both in area, size and the number of neurons (**C** *kl*/*kl* mice, **D** WT mice). Large AHCs are seen more frequently in WT mice (**F**) than in *kl*/*kl* mice (**E**), and small neurons are seen more frequently in the anterior horn in *kl*/*kl* mice (**E**) than in WT mice (**F**). The amount of Nissl substance in the AHCs in *kl*/*kl* mice is less than that in WT mice, indicating chromatolysis by the *klotho* insufficiency (**G**). Accumulation of phosphorylated neurofilaments is observed in the AHCs of *kl*/*kl* mice (**I**) as compared with the WT mice (**J**). GFAP-immunopositive reactive gliosis is seen in the ventral horn of *kl*/*kl* mice (**K**) as compared with WT mice (**L**). There is no significant difference in the number of neurons in the ventral part of the spinal gray matter between *kl*/*kl* mice (*open bar*) and WT mice (*hatched bar*) (*error bars* indicate SD) (**H**) (*AHC* anterior horn cell, *GFAP* glial fibrillary acidic protein). **A**–**G** Klüver-Barrera staining; **I**, **J** SMI-31-immunohistochemistry; **K**, **L** GFAP immunohistochemistry. *Bars* **A**, **B** 0.5 mm; **C**, **D**, **G**, **I**, **J** 25 μm; **E**, **F**, **K**, **L** 50 μm

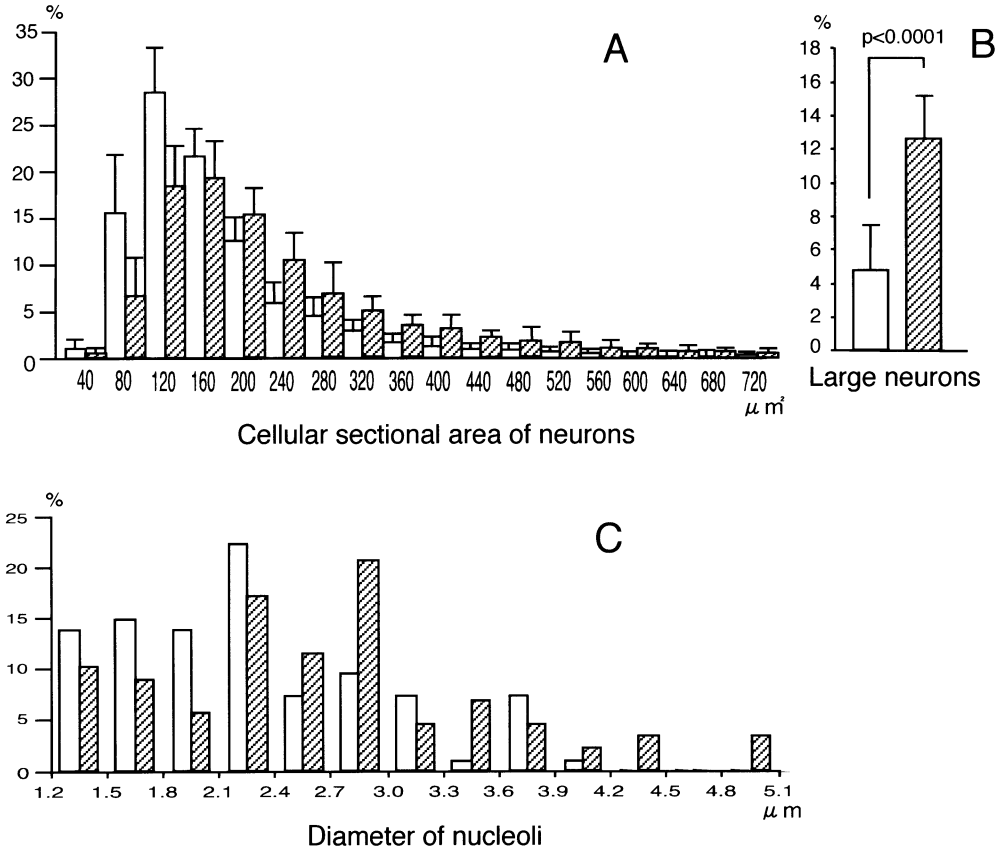

Fig. 3 Distribution of the sectional area of the neurons in the ventral gray matter of the 5th cervical cord. The frequency distribution of the sectional area of the neurons shows one peak at 120 μm^2 in *kl*/*kl* mice but 160 μm^2 in WT mice, indicating smaller neurons in the *kl*/*kl* mice (**A**). The number of large neurons with a cross-sectional area over 400 μm^2 is significantly lower in *kl*/*kl* mice than WT mice (**B**). The frequency distribution by 0.3-μm increments of the diameter of nucleoli of neurons in the ventral spinal gray matter shows the highest peaks at 2.1–2.4 μm in *kl*/*kl* mice but at 2.7–3.0 μm in WT mice (**C**). *Open bars*: *kl*/*kl* mice, *hatched bars*: WT mice, *error bars*: SD

WT mice (Fig. 3C). The diameter of neuron nuclei in the ventral spinal gray matter was 2.50 ± 0.91 μm (mean ± SD) in *kl*/*kl* mice and 2.67 ± 0.77 μm in WT mice; those in *kl*/*kl* mice were significantly smaller ($P < 0.01$).

Amount of cytoplasmic RNA in AHCs

The integrated OD value of the cytoplasmic RNA in the large AHCs stained with pyronin Y in *kl*/*kl mice* was 64.4% of that seen in the WT mice (Table 2, Fig. 4).

Ultrastructural findings of the AHCs

For *kl*/*kl* mice, the rER was severely fragmented, and the size of cisternae of the rER was reduced. The number of the attached and free ribosomes was noticeably reduced in the AHCs as compared to those in WT mice, while mitochondria, nuclear membrane, karyoplasm and nucleolus in the AHCs in these mice appeared normal (Fig. 5A, B).

Table 2 The integrated optical density values (mean ± SD) of the cytoplasmic RNA in the large AHCs stained with pyronin Y in *kl*/*kl* and WT mice. Measurement was performed in 100 randomly distributed AHCs with nucleolus (10 AHCs/mouse,10 mice each) (*AHC* anterior horn cell)

	Integrated OD value
kl/*kl* (male)	5,424 ± 3,450* ($n = 100$)
WT (male)	8,427 ± 6,988 ($n = 100$)

*$P < 0.05$

Transcription activity of rRNA gene in the AHCs

AgNOR-positive areas were clearly and exclusively observed in dark fine granules within the nucleus and in the nucleolus. The ratios of AgNOR-positive areas to cross-sectional areas of the nucleus were significantly lower in the neurons of *kl*/*kl* mice than of WT (Fig. 6A–C).

Discussion

The *klotho* gene carries two varieties of mRNA. The majority is mRNA coding a membrane-type Klotho protein, from which a transmembrane-type Klotho protein is translated [27, 29]. The transmembrane-type protein is composed of an N-terminal signal sequence and a C-terminal transmembrane domain, and between them, two domains (KL1, KL2) homologous to β-glucosidase hydrolyzing steroid β-glucuronides [39]. The other mRNA variety gives rise to strap codons, which translate an approximately half-length secretory Klotho

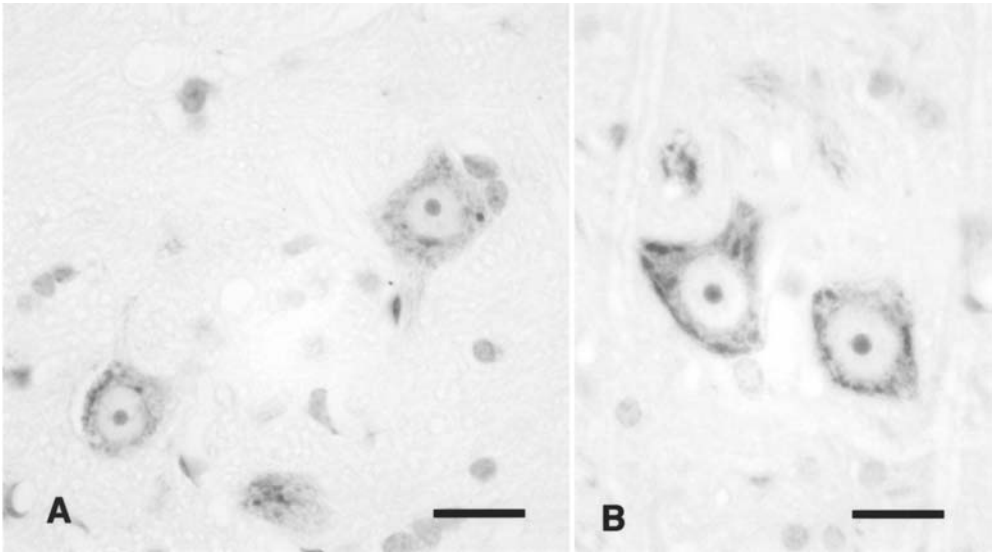

Fig. 4 Pyronin Y-stained AHCs in *kl*/*kl* (**A**) and WT (**B**) mice. *Bars* 20 μm

protein. The secretory Klotho protein has only a signal sequence and KL1 domain. It is not known whether Klotho proteins have enzymatic activity. The *klotho* gene is reported to be strongly expressed in the kidneys, and weakly in the brain. *Klotho* gene expression has not been reported in the lungs, bones, or skin, which show severe pathological changes in *kl*/*kl* mice. These facts suggest the possibility that pathological findings in *kl*/*kl* mice are not a simple phenotype of the *klotho* gene, but that the secretory Klotho protein may have some function whereby pathological changes are suppressed in WT mice [27, 29].

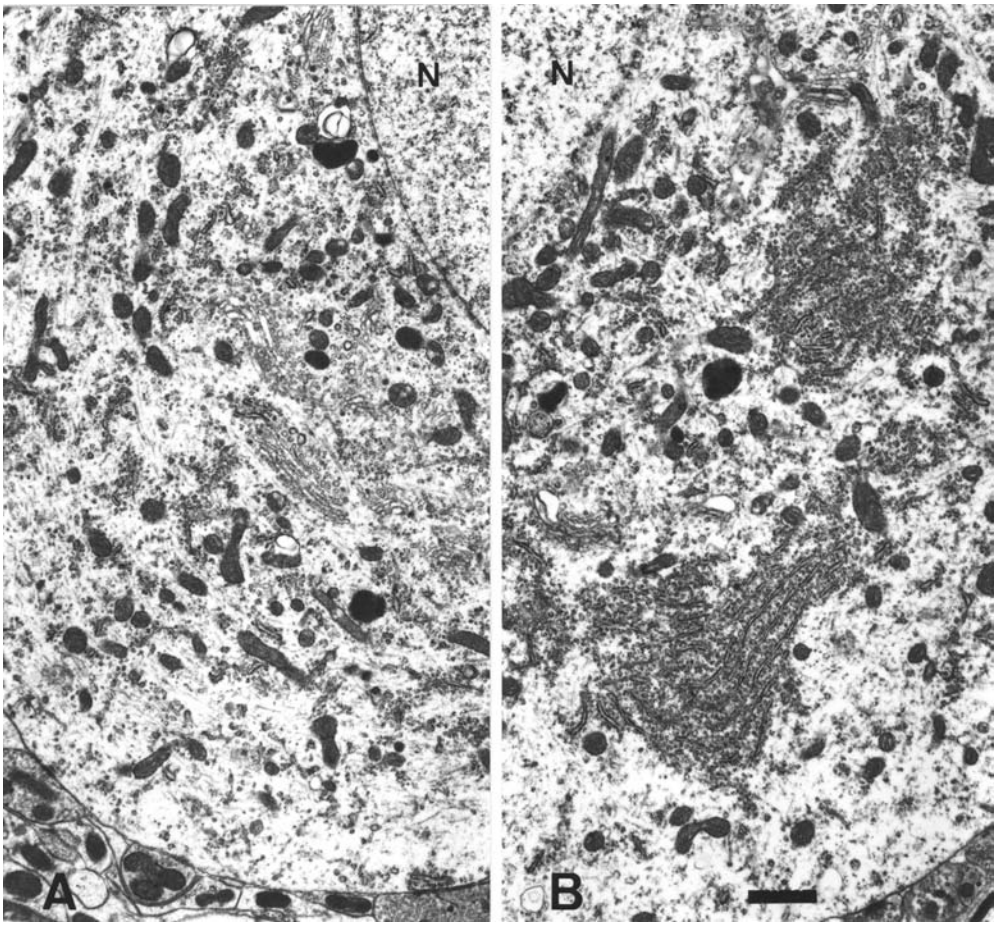

Fig. 5 Ultrastructure of the AHCs. The rERs are severely fragmented, and the amount of rER and the number of free ribosomes sre obviously lower in the neurons of *kl*/*kl* mice (**A**) as compared with those in WT mice (**B**), whereas mitochondria, nuclear membrane, and nuclear karyoplasm and nucleolus in the AHCs in *kl*/*kl* mice appear unchanged (*rER* rough endoplasmic reticulum, *N* nucleus). Uranyl-lead staining. *Bar* 1 μm

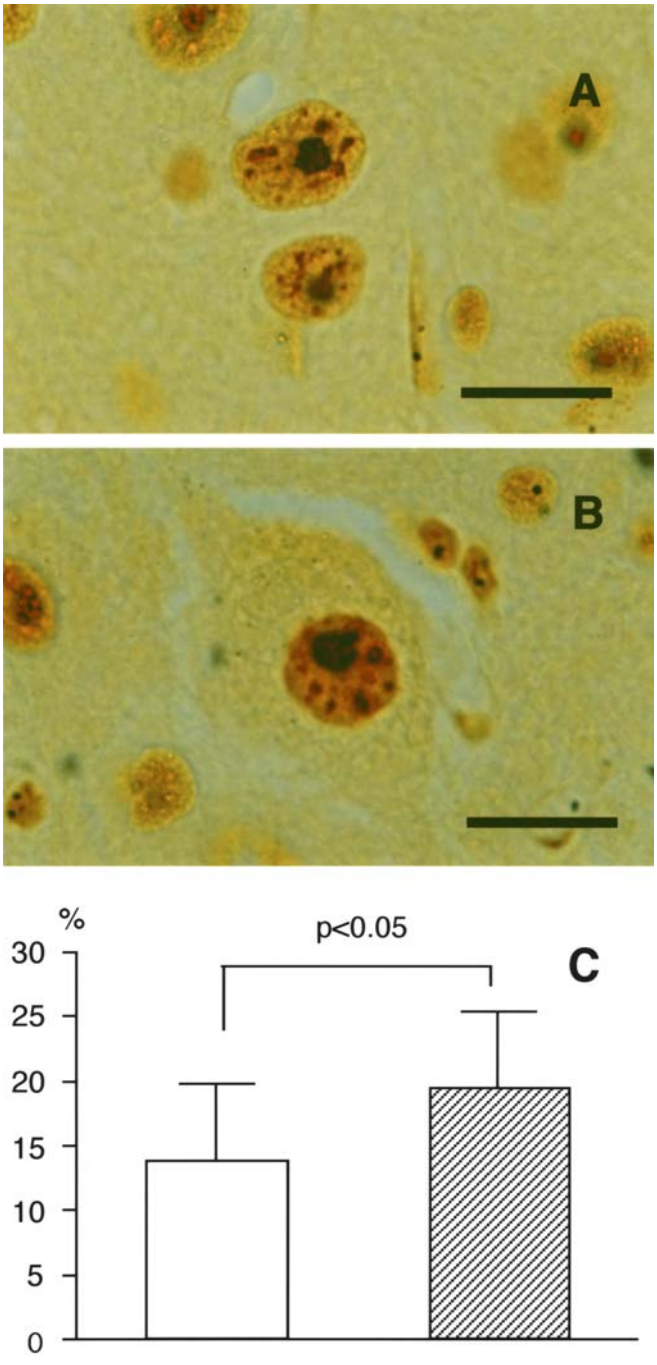

Fig. 6 Transcription activity of rRNA gene in the AHCs. AgNOR-positive area in large AHCs of the *kl*/*kl* mice (**A**) and WT mice (**B**). The ratio of this area to cross-sectional cellular area of the nucleus is significantly lower in *kl*/*kl* mice (*open bar*) than WT mice (*hatched bar*) (*error bars* indicate SD) (**C**) (*rRNA* ribosomal RNA, *AgNORs* Silver staining of nucleolar organizer region-associated proteins)

Our present investigation on *klotho* gene expression revealed that the gene was observed strongly in WT and weakly, but significantly, in *kl*/*kl* mice after 40 cycles in RT-PCR in the spinal cord. This result demonstrates that *kl*/*kl* mice are not null but severe hypomorph mice of the Klotho protein, and that the decrease of this protein may induce various morphological alterations observed in the present study.

The differential AgNOR staining is believed to stain certain proteins combined specifically with an rRNA gene, and the quantity of the proteins (AgNOR-positive areas) is believed to reflect the transcription activity of the rRNA gene [4, 6, 14]. To date, AgNOR stainability has been reported to be an index of phenomena including protein synthesis [4, 12], tumor proliferation [7, 8, 11, 31, 32, 34, 43], long-term changes during development [12], brain augmentation due to learning [42], decline in the aging brain [22, 23], and age-related reduction among dermal fibroblasts [8, 38].

The present light microscopic study showed a loss of Nissl substance (chromatolysis) in the AHCs of *kl*/*kl* mice. Reduction of integrated OD value of pyronin Y-positive material in the cytoplasm of AHCs in *kl*/*kl* mice indicates a decrease of the cytoplasmic RNA content, and ultrastructural investigation of AHCs revealed a reduction of the number of attached and free ribosomes and of rER in the mice in the present study. The ratio between the activity of rRNA gene transcription and the size of the nucleus in the anterior horn cells were evaluated. The results indicated that the depletion of the activity of rRNA gene transcription was not proportional to overall cell size. Thus, decreased transcription activity of the rRNA gene in the spinal neurons observed in the present study may cause a decrease in cytoplasmic RNA, ribosomes and rER of the AHCs. The reduction of the amount of the ribosomes and rER might induce small neurons in the AHCs of the spinal cord with sparing the posterior horn in *kl*/*kl* mice. To determine the cause and mechanism, the amount of Klotho protein should be examined both in the ventral and posterior horns. In addition, regarding the mechanism of reduction of rRNA gene transcription activity, it should be elucidated whether or not the rRNA gene decreases in the chromosomal DNA; some genes are unavailable in the hybridization after being covered by proteins or other cross-linkers [13], and the RNA polymerase I, TFIIA, TFIIB, TATA box-binding protein, and CRE-binding protein exist normally in the AHCs [2].

A decreased number of small neurons and the absence of chromatolysis have been reported in the AHCs of aged humans [5, 26, 37, 40]. These findings differ from those observed in the *kl*/*kl* mice in the present study. Thus, the pathological mechanisms occurring in the spinal cord in aged humans and *kl*/*kl* mice are considered to be basically dissimilar. Further examination of the spinal cords in fetus and newborn, to analyze possibly overlapping developmental disturbance, is needed to determine the cause of the severe reduction in the volume of the spinal cord in *kl*/*kl* mice.

Kl/*kl* mice show a marked reduction in body weight. Thus, developmental retardation may exist in the mice. However, the brain is relatively well developed and preserved. Neuronal population and the size of neurons in the brains did not show any apparent differences from

those of the controls. In addition, the number and size of the neurons in the posterior horn in the spinal cord appeared to be preserved. These findings indicate that normal development and selective degeneration possibly occurred in the AHCs. It is hardly conceivable that selective developmental retardation occurred in the AHCs, and that developmental retardation of the skeletal muscles induce anterior horn degeneration showing rER reduction. There have been no reports that any congenital muscle dystrophy in mice or humans induces rER reduction in the AHCs.

On the other hand, a decreased number of large neurons and reduced amount of the cytoplasmic RNA, rER and ribosomes, as observed in the spinal cord of *kl*/*kl* mice, have been noted in the motor neurons in the spinal cord and brain stem of patients with classic ALS [15, 16, 28]; however, Bunina bodies and spheroids were absent in these mice. An accumulation of neurofilaments in the AHCs, as in patients with classic ALS [9, 24, 35], was also reported in the peripheral nerve axon in *kl*/*kl* mice [41]. Decrease of rER (chromatolysis) and accumulation of neurofilaments have been considered to be early changes in the AHCs in patients with classic ALS [17, 20]. Reactive astrocytosis observed in the anterior horn of the *kl*/*kl* mice in the present study relates to a degenerative process, and has been reported in the ventral horn in patients with classic ALS. This resemblance shows that *klotho* gene insufficiency causes neuronal dysfunction, and might indicate that the *klotho* gene is involved in the pathological mechanism of classic ALS. Mutant SOD mice may be a good tool for the research of familial ALS [10], and further study is needed to evaluate whether the *kl*/*kl* mice, which are senescence-accelerated mice showing decreased rER, ribosomes, and cytoplasmic RNA in the AHCs, is a new animal model of AHC degeneration, and can provide clues to understanding the etiology of classic ALS.

Acknowledgements The authors are indebted to Dr. K. Watabe of the Department of Molecular Neuropathology, and Dr. J. Kimura-Kuroda and Dr. I. Nagata (Department of Brain Structure, Tokyo Metropolitan Institute for Neuroscience), Dr. K. Honma (Graduate School of Pharmaceutical Science, University of Tokyo), Ms. M. Shinohara (Department of Anatomy, School of Veterinary Medicine, Tokyo University of Agriculture and Technology), and Dr. A. Mabuchi (Department of Orthopedic Surgery, Graduate School of Medicine, University of Tokyo) for their help during the research. This work was supported in part by grants from the Japanese Ministry of Health, Labor and Welfare (to Y.N., and Research on Psychiatric and Neurological Diseases and Mental Health (H16-kokoro-017 to K.O.)); the Japanese Ministry of Education, Science, Sports and Culture (nos. 12137201 to H.K., 12307031 to K.N., 14657376 to E.K. and 14580735 to K.O.) and the Japan Space Forum (to H.K.).

References

1. Abercrombie M (1946) Estimation of nuclear population from microtome sections. Anat Rec 94:239–247
2. Alberts B, Bray D, Johnson A, Lewis J, Raff M, Roberts K, Walter P (1998) Essential cell biology. Garland, New York
3. Arking DE, Becker DM, Yanek LR, Fallin D, Jdge DP, Moy TF, Becker LC, Dietz HC (2003) KLOTHO allele status and the risk of early-onset occult coronary artery disease. Am J Hum Genet 72:1154–1161
4. Babu KA, Verma RS (1985) Structural and functional aspects of nucleolar organizer regions (NORs) of human chromosomes. Int Rev Cytol 94:151–171
5. Bailey AA (1953) Changes with age in the spinal cord. Arch Neurol Psychiatry 70:299–309
6. Baldini A, Marleka P (1985) Hormone-modulated rRNA gene activity is visualized by selective staining of the NOs. Cell Biol Int Rep 9:791–796
7. Brustmann H, Riss P, Naude S (1995) Nucleolar organizer regions as markers of endometrial proliferation: a study of normal, hyperplastic, and neoplastic tissue. Hum Pathol 26:664–667
8. Buys CHCM, Osinga J, Anders GJPA (1979) Age-dependent variability of ribosomal RNA-gene activity in man as determined from frequencies of silver staining nucleolus organizing regions of metaphase chromosomes of lymphocytes and fibroblasts. Mech Ageing Dev 11:55–75
9. Carpenter S (1968) Proximal axonal enlargement in motor neuron disease. Neurology 18:841–851
10. Cleveland DW, Rothstein JD (2001) From Charcot to Lou Gehrig: deciphering selective motor neuron death in ALS. Nat Rev Neurosci 2:806–8199
11. Crocker J, Boldy DAR, Egan MJ (1989) How should we count AgNORs? Proposals for a standardized approach. J Pathol 158:185–188
12. Fushiki S, Kinoshita C, Tsutsumi Y, Nishizawa Y (1995) Age-related changes of the argyrophilic nucleolar organizer regions in mouse neocortical neurons. Acta Histochem Cytochem 28:533–538
13. Gaubatz J, Cutler RG (1978) Age-related differences in the number of ribosomal RNA genes of mouse tissue. Gerontology 24:179–207
14. Goodpasture C, Bloom SE (1975) Visualization of nucleolar organizer regions in mammalian chromosomes using silver staining. Chromosoma 53:37–50
15. Hartmann HA, McMahon S, Sun DY, Abbs JH, Uemura E (1989) Neural RNA in nucleus ambiguous and nucleus hypoglossus of patients with amyotrophic lateral sclerosis. J Neuropathol Exp Neurol 48:669–673
16. Hirano A (1991) Cytopathology of amyotrophic lateral sclerosis. Adv Neurol 56:91–101
17. Hirano A, Inoue K (1980) Early pathological changes of amyotrophic lateral sclerosis. Electron microscopic study of chromatolysis, spheroids and Bunina bodies. Neurol Med 13:148–160
18. Howell WM, Black DA (1980) Controlled silver staining of nucleolus organizer regions with a protective colloidal developer: a 1-step method. Experientia 36:1014–1015
19. Hubbell HR (1985) Silver staining as an indicator of active ribosomal genes. Stain Technol 60:285–294
20. Inoue K, Hirano A (1979) Early pathological changes of amyotrophic lateral sclerosis. Autopsy findings of a case of 10 months' duration. Neurol Med 11:448–455
21. Jimenez R, Burgos M, Diaz de la Guardia R (1988) A study of the Ag-staining significance in mitotic NORs. Heredity 60:125–127
22. Johnson R, Stehler BL (1972) Loss of genes coding for ribosomal RNA in ageing brain cells. Nature 240:412–414
23. Johnson RW, Chrisp C, Stehler BL (1972) Selective loss of ribosomal RNA genes during the ageing of post-mitotic tissues. Mech Ageing Dev 1:183–198
24. Julien JP (1995) A role for neurofilaments in the pathogenesis of amyotrophic lateral sclerosis. Biochem Cell Biol 73:593–597
25. Kameyama T, Hashizume Y, Sobue G (1996) Morphologic features of the normal human cadaveric spinal cord. Spine 21:1285–1290

26. Kawamura Y, O'Brien P, Okazaki H Dyck PJ (1977) Lumbar motoneurons of man. II. The number and diameter distribution of large-and intermediate-diameter cytons in "motoneuron columns" of spinal cord of man. J Neuropathol Exp Neurol 36:861–870
27. Kuro-o M, Matsumura Y, Aizawa H, Kawaguch H, Suga T, Utsugi T, Ohyama Y, Kurabayashi M, Kaname T, Kume E, Iwasaki H, Iida A, Shiraki-Iida T, Nishikawa S, Nagai R, Nabeshima Y (1997) Mutation of the klotho gene leads to a syndrome resembling ageing. Nature 390:45–51
28. Mann DMA, Yates PO (1974) Motor neuron disease: the nature of the pathogenic mechanism. J Neuropathol Exp Neurol 37:1036–1046
29. Matsumura Y, Aizawa H, Shiraki-Iida T, Nagai R, Kuro-o M, Nabeshima Y (1998) Identication of the human klotho gene and its two transcripts encoding membrane and secreted Klotho protein. Biochem Biophys Res Commun 242:626–630
30. Morton CC, Brown JA, Holmes WM, Nance WE, Wolf B (1983) Stain intensity of human nucleolus organizer region reflects incorporation of uridine into mature ribosomal RNA. Exp Cell Res 145:405–413
31. Nielsen AL, Nyholm HC, Engel P (1994) Expression of MIB-1 (Paraffin ki-67) and AgNOR morphology in endometrial adenocartinomas of endometrioid type. Int J Gynecol Pathol 13:37–44
32. Niwa K, Yokoyama Y, Tanaka T, Mori H, Mori H, Tamaya T (1991) Silver-stained nucleolar organizer regions in the normal, hyperplastic and neoplastic endometrium. Virchows Arch [A] 29:493–497
33. Rexed B (1952) The cytoarchitectonic organization of the spinal cord in the cat. J Comp Neurol 96:415–495
34. Ruschoff J, Plate K, Bittinger A, Thomas C (1989) Nucleolar organizer regions (NORs). Basic concepts and practical application on tumor pathology. Pathol Res Pract 185:878–885
35. Schmidt M L, Carden MJ, Lee VM, Trojanowski JQ (1987) Phosphate dependent and independent neurofilament epitopes in the axonal swellings of patients with motor neuron disease and controls. Lab Invest 56:282–294
36. Schulte EK, Lyon HO, Hoyer PE (1992) Simultaneous quantitafication of DNA and RNA in tissue sections. A comparative analysis of the methyl green-pyronin technique with the gallocyanin chromalum and Feulgen procedures using image cytometry. Histochem J 24:305–310
37. Terao S, Sobue G, Hashizume Y, Li M, Inagaki T, Mitsuma T (1996) Age-related changes in human spinal ventral horn cells with special reference to the loss of small nerurons in the intermediate zone: a quantitative analysis. Acta Neuropathol 92:109–114
38. Thomas S, Mukherjee AB (1996) A longitudinal study of human age-related ribosomal RNA gene activity as detected by silver-stained NORs. Mech Ageing Dev 92:101–109
39. Tohyama O, Imura A, Iwao A, Freund JN, Henrissat B, Fujimori T, Nabeshima Y (2004) Klotho is a novel beta-glucuronidase capable of hydrolyzing steroid beta-glucuronides. J Biol Chem 279:9777–9784
40. Tomlinson BE, Irving D (1977) The number of limb motor neurons in the human lumbosacral cord throughout life. J Neurol Sci 34:213–219
41. Uchida A, Komiya Y, Tashiro T, Yorifuji H, Kishimoto T, Nabeshima Y, Hisanaga S (2001) Neurofilaments of Klotho, the mutant mouse prematurely displaying symptoms resembling human aging. J Neurosci Res 64:364–370
42. Vargas JP, Rodríguez F, Lépez JC, Arias JL, Salas C (2000) Spatial learning-induced increase in the argyrophilic nucleolar organizer regions of dorsolateral telencephalic neurons in goldfish. Brain Res 865:77–84
43. Wilkinson N, Buckley H, Chawner L, Fox H (1990) Nucleolar organizer regions in normal, hyperplastic, and neoplastic endometria. Int J Gynecol Patho l 9:55–59